

Equilibrium, Kinetic and Thermodynamic Studies on the Adsorption of Direct Dye onto a Novel Green Adsorbent Developed from *Uncaria Gambir* Extract

Azraa Achmad*, Jain Kassim, Tong Kim Suan, Rozaini Che Amat and Tan Lean See

School of Chemical Sciences,
Universiti Sains Malaysia, 11800 USM Pulau Pinang, Malaysia

*Corresponding author: aa09_che029@student.usm.my

Abstract: *Uncaria gambir* extract was chemically modified for the purpose of developing a novel green adsorbent. The modified gambir adsorbent was characterised by FTIR, SEM-EDX and pH_{zpc} , and its potential for the removal of Direct Red 23 from aqueous solution was investigated. The results showed that the equilibrium data were well described by the Langmuir isotherm model, with a maximum adsorption capacity of 26.67 mg/g. The kinetics of adsorption of Direct Red 23 followed a pseudo-second-order kinetic model. Thermodynamic parameters such as enthalpy change (ΔH°), free energy change (ΔG°) and entropy change (ΔS°) were studied, and the adsorption process of Direct Red 23 was found to be endothermic and spontaneous.

Keywords: *Uncaria gambir*, Direct Red 23, Langmuir, pseudo-second-order, thermodynamic

1. INTRODUCTION

It is estimated that approximately 40,000 tonnes of dyes out of roughly 450,000 tonnes in total production are not used but discharged into wastewaters. A large variety of dyestuffs is available under the categories of acid, basic, reactive, direct, disperse, sulphur and metallic dyes.¹ Dyes are synthetic aromatic compounds, which have various functional groups.² Some dyes and their degradation products may be carcinogens and toxic, and consequently their treatment cannot depend on biodegradation alone.^{3,4} Therefore, extensive research has been conducted to find an effective and efficient alternative for the removal of dyes.

Adsorption is one of the most common methods used in wastewater treatment because it is economical, effective and simple in design. However, the adsorption process is influenced by the nature of the adsorbate and its substituent groups. The presence and concentration of surface functional groups play an important role in the adsorption capacity and the removal mechanism of the adsorbate.^{5,6}

The most commonly used adsorbent in the adsorption process is activated carbon. Activated carbon has the advantage of exhibiting a high adsorption capacity for colour pollutants due to their high surface area and porous structure.⁷ Although activated carbon is an effective and efficient adsorbent, its application is limited due to high cost and minimal decomposition, which may cause more environmental problems.^{8,9} Therefore, alternative low-cost adsorbents such as chitin,¹⁰ coffee,¹¹ tea waste,¹² orange peel,¹³ rice husk,¹⁴ bark¹⁵ and coir pith¹⁶ have been studied.

Uncaria gambir (gambir), a native Southeast Asian herbal plant, can be mostly found in countries such as Indonesia and Malaysia. It has been widely used as an astringent medicine and for tanning, calico printing and dyeing purposes. *Uncaria gambir* consists mostly of flavanol monomers such as (+)-catechin, (+)-epicatechin and alkaloids.¹⁷

The aim of this research was to produce a novel adsorbent from *Uncaria gambir*. The gambir adsorbent was characterised by Fourier Transform Infrared (FTIR) spectroscopy, Scanning Electron Microscopy (SEM) with Energy Dispersive X-ray (EDX) analysis and pH zero of point charge (pH_{zpc}) method. The equilibrium data were analysed using Langmuir, Freundlich and Temkin adsorption isotherm models. Kinetics was also evaluated using pseudo-first-order, pseudo-second-order and intraparticle diffusion models. Thermodynamic parameters were studied to determine the adsorption process of Direct Red 23 onto the modified gambir adsorbent.

2. EXPERIMENTAL

2.1 Preparation of the Adsorbate

Direct Red 23 (C.I. 29160, ALDRICH, SIGMA-ALDRICH, Selangor, Malaysia. 30% dye content, chemical formula = C₃₅H₂₅N₇Na₂O₁₀S₂, FW = 813.74 and λ_{max} = 510 nm) was used without further purification. The stock solution of Direct Red 23 (500 mg/l) was prepared by dissolving 0.25 g of direct red 23 with distilled water in a 500 ml volumetric flask. Experimental solutions of the desired concentration were prepared by diluting the stock solution with distilled water.

2.2 Preparation of the Modified Gambir Adsorbent (MGA)

Uncaria gambir cubes were ground and sifted through a 250 μm sieve. Initially, the gambir powder was defatted with n-hexane and then extracted with ethyl acetate (3 \times 50 ml). The collected solvent was evaporated and dried in an oven to obtain the powder form of the gambir extract. In a 50 ml round bottom

flask, 0.1 g of gambir extract was added to 10 ml of distilled water, 2 ml of 37% formaldehyde and 1 ml of 10 M HCl. The round bottom flask was attached to a condenser and refluxed at 90°C for 1 hour. After reflux, the modified gambir extract was filtered out and washed with hot distilled water until the pH of the filtrate was approximately 4. The MGA was dried in an oven at 50°C for further adsorption analyses.

2.3 Characterisation of the MGA

The FTIR spectra of the unloaded MGA and the MGA loaded with Direct Red 23 were recorded by a Perkin Elmer FTIR System 2000 Model spectrometer. The spectra were analysed in the range of 400–4000 cm^{-1} . SEM with EDX analysis of the MGA was performed to study the surface texture of the MGA. The pH_{zpc} of the MGA was determined by using the batch equilibrium method with some modification. In conical flasks, 0.15 g of the MGA was added to a 0.1 M KNO_3 solution in each flask, and the solutions were adjusted from pH 2 to 10 by adding 0.5 M HCl or 0.5 M NaOH. The mixtures were stirred at 100 rpm for 24 hours at room temperature. The final pH of the mixtures was measured after 24 hours.

2.4 Batch Adsorption Studies

For isotherm studies, the effect of the initial Direct Red 23 concentration (25 and 300 mg/l) was investigated by adding 0.2 g of the MGA into 50 ml of each Direct Red 23 solution, and the solutions were adjusted to pH 2.0 with 0.1 M HCl. The mixtures were agitated at 100 rpm for 2 hours. For the kinetics study, the experiments were conducted by adding 0.2 g of the MGA into 50 ml of the Direct Red 23 solutions (50 mg/l and 100 mg/l) and agitated for varying contact times (5 min to 120 min) at room temperature. The thermodynamic study was conducted at different temperatures (303 to 333 K). The final concentrations of the Direct Red 23 solutions were analysed using a UV–VIS spectrophotometer (JASCO V-530, JASCO, USA). The percentage of Direct Red 23 removed by the MGA was calculated by the following equation:

$$\% \text{ Removal} = \frac{C_0 - C_e}{C_0} \times 100 \quad (1)$$

The amount of Direct Red 23 adsorbed at equilibrium, q_e (mg/g), was calculated using the following equation:

$$q_e = \frac{(C_0 - C_e)V}{M} \quad (2)$$

where C_0 and C_e (mg/l) are the initial and equilibrium concentrations of Direct Red 23, respectively, V (l) is the volume of the Direct Red 23 solution and M (g) is the adsorbent mass.

3. RESULTS AND DISCUSSION

3.1 Characterisation of Gambir Adsorbent

The FTIR spectrum of the MGA is shown in Figure 1. The broad band that falls in the range of $3500\text{--}3200\text{ cm}^{-1}$ is associated with the --OH group. The peaks at 1614 cm^{-1} and 1521 cm^{-1} correspond to the C=C stretching vibration. The peak observed at 1457 cm^{-1} can be attributed to the formation of methylene bridges from the reaction of the phenolic groups with formaldehyde.¹⁸ The peaks at the regions 1290 cm^{-1} , 1239 cm^{-1} and 1115 cm^{-1} correspond to the C-O stretching. Generally, the FTIR spectrum for the modified gambir adsorbent indicated the presence of the hydroxyl functional group, --OH , which might be responsible for the adsorption of Direct Red 23. Figure 2 shows the suggested adsorption mechanism between the hydroxyl (--OH) group of the MGA and the sulphonate (--SO_3^-) group of Direct Red 23. The --OH group of the MGA was protonated due to the low pH of the solution. The presence of the --SO_3^- group in Direct Red 23 will preferentially favour the protonated --OH group of the MGA to form a hydrogen bond during the adsorption process.

Figure 3 shows the SEM micrograph of the MGA, which has considerable porous, granular and almost uniform in size where Direct Red 23 could be adsorbed with a high probability. The EDX spectra of the MGA consist of C and O elements. The presence of Au in both spectra is due to the gold coating used to increase the electric conduction and improve the image quality.¹⁹ The pH_{zpc} of the MGA was measured to be 3.50. The pH_{zpc} of an adsorbent is a very important characteristic that indicates the pH at which the adsorbent is neutral, whereas beyond this pH, the adsorbent becomes either positively or negatively charged. The result shows that the MGA was positively charged on its surface below pH 3.50, and it favoured the adsorption of Direct Red 23.

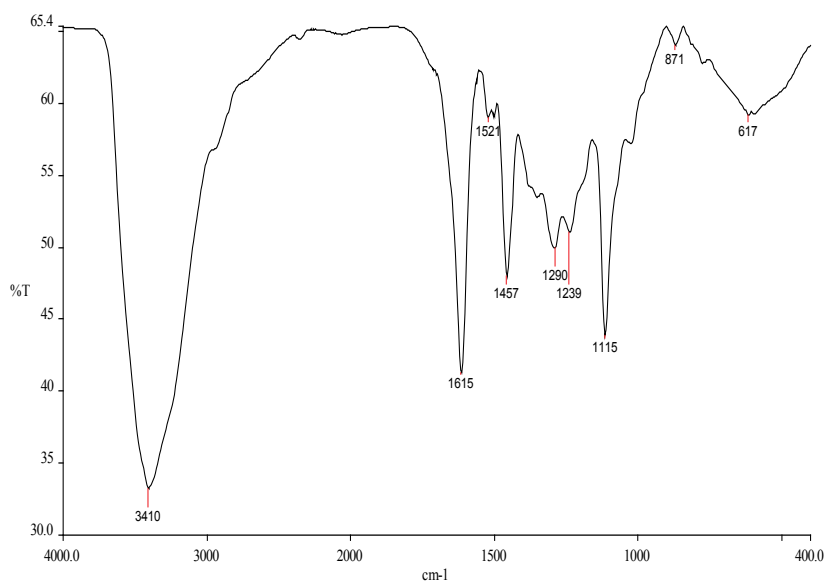


Figure 1: Fourier Transform Infrared (FTIR) spectra of modified gambir adsorbent (MGA).

3.2 Adsorption Isotherm

The Langmuir and Freundlich equations were used to study the interaction between Direct Red 23 and the modified gambir adsorbent. The Langmuir equation can be written in the following linear form:²⁰

$$C_e/q_e = 1/(q_m K_L) + C_e/q_m \quad (3)$$

where C_e (mg/l) is the concentration of Direct Red 23 at equilibrium, K_L (l/mg) is the Langmuir constant related to the adsorption energy and q_m (mg/g) is the adsorption capacity. The adsorption capacity can be correlated with the variation of the surface area and porosity of the adsorbent. Higher surface area and pore volume will result in higher adsorption capacity.¹⁶ The essential characteristics of the Langmuir isotherm can be expressed by a dimensionless constant called the equilibrium parameter, R_L .²¹

$$R_L = 1/(1 + K_L C_0) \quad (4)$$

where K_L (mg/l) is the Langmuir constant and C_0 (mg/l) is the initial Direct Red 23 concentration, with R_L values indicating the type of isotherm. The R_L value indicates the adsorption to be unfavourable ($R_L > 1$), linear ($R_L = 1$), favourable

($0 < R_L < 1$) or irreversible ($R_L = 0$). The R_L value obtained from the experimental data is between zero and one, indicating favourable adsorption.

The Freundlich equation can be written in the following linear form:²²

$$\log q_e = \log K_F + 1/n \log C_e \quad (5)$$

where K_F (L/g) is the Freundlich constant related to the adsorption capacity and n is the constant for intensity. The value of $1/n$ ranging between 0 and 1 is a measure of adsorption intensity or surface heterogeneity and becomes more heterogeneous as its value gets closer to zero.¹²

The Temkin isotherm has generally been applied in the following form:²³

$$q_e = B_T \ln A_T + B_T \ln C_e \quad (6)$$

where $B_T = RT/b_T$, T (K) is the absolute temperature, R (8.314 J/mol) is the universal gas constant, A_T (1/mg) is the equilibrium binding constant and b_T (J/mol) is related to the heat of adsorption. The isotherm constants A_T and b_T are calculated from the slope and intercept of the q_e versus $\ln C_e$ plot.

The Langmuir, Freundlich and Temkin isotherm constants are presented in Table 1. From Table 1, it can be seen that the regression correlation coefficient (R^2) of the Langmuir equation ($R^2 = 0.9926$) is more linear when compared with that of the Freundlich equation ($R^2 = 0.9582$) and the Temkin equation ($R^2 = 0.9700$), implying that the adsorption isotherm data are well fitted by the Langmuir isotherm. The monolayer adsorption capacity, according to the Langmuir isotherm, was found to be 26.67 mg/g at 30°C. The fact that the Langmuir isotherm fits the experimental data very well may be due to the homogeneous distribution of active sites on the MGA surface because application of the Langmuir equation involves the assumption that the surface is homogeneous.

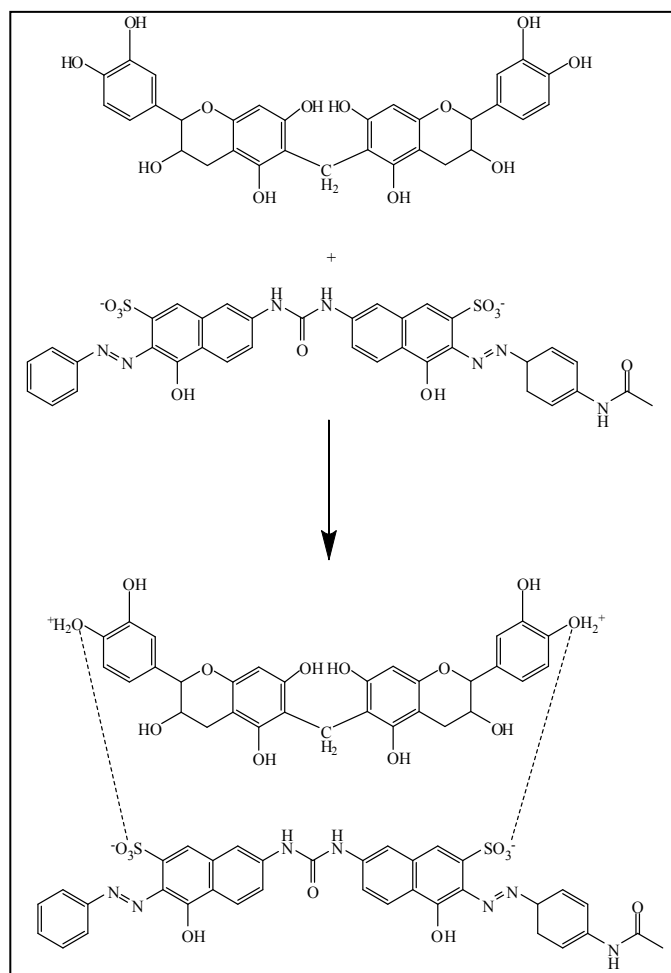


Figure 2: The suggested mechanism for the adsorption of Direct Red 23 onto MGA.

Table 1: Adsorption isotherm constants for adsorption of Direct Red 23 onto gambir adsorbent.

Langmuir isotherm			Freundlich isotherm			Temkin isotherm		
q_m (mg/g)	K_L (l/mg)	R^2	K_F (mg/g)	1/n	R^2	b_T (kJ/mol)	A_T (dm ³ /mol)	R^2
26.67	0.11	0.9926	8.18	0.23	0.9582	767.38	11.28	0.9700

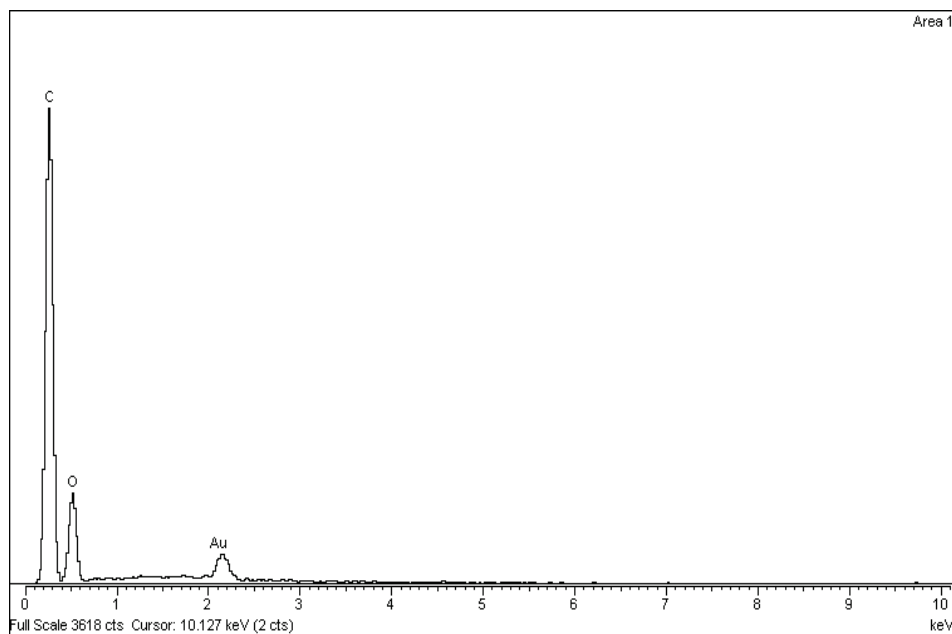
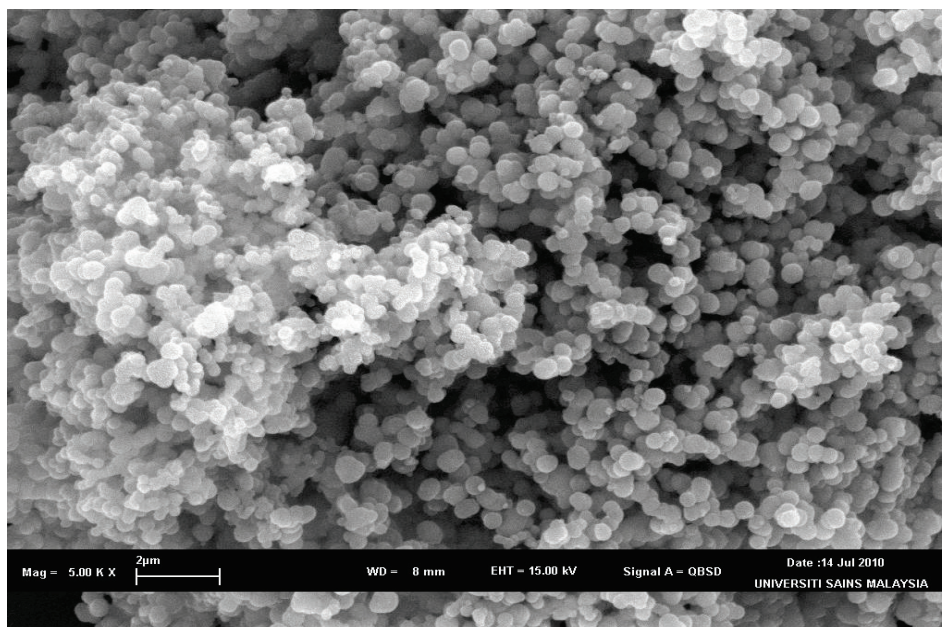


Figure 3: Scanning Electron Microscopy (SEM) with Energy Dispersive X-ray (EDX) spectra of MGA.

3.3 Adsorption Kinetics

The adsorption mechanism of Direct Red 23 onto the MGA was studied using pseudo-first-order and pseudo-second-order kinetic equations. The pseudo-first-order kinetic equation is given as:

$$\log(q_e - q_t) = \log q_e - \frac{k_1}{2.303}t \quad (7)$$

where q_e and q_t (mg/g) are the amount of Direct Red 23 adsorbed on the MGA at equilibrium and at time t (min), respectively. k_1 (1/min) is the pseudo-first-order rate constant.

The pseudo-second-order kinetic equation is described as:

$$\frac{t}{q_t} = \frac{1}{k_2 q_e^2} \frac{1}{q_e} t \quad (8)$$

where k_2 (g/mg min) is the rate constant and q_e and q_t (mg/g) are the amount of Direct Red 23 adsorbed on the MGA at equilibrium and at time t (min), respectively.

To study the diffusion mechanism of adsorption, the kinetic results were evaluated using the intraparticle diffusion model.²⁴ During the intraparticle diffusion process, the adsorbate species are most probably transferred from the bulk of the solution into the solid phase.²⁵

The intraparticle diffusion equation is given as:²⁶

$$q_t = K_p t^{0.5} + C \quad (9)$$

where K_p (mg/g min^{0.5}) is the intraparticle diffusion rate constant and C is the intercept. The boundary layer thickness is described by the values of the intercept. The larger the intercept, the greater is the boundary layer effect.²⁷ As seen in Table 2, the correlation coefficient R^2 for the pseudo-second-order kinetic model is greater than 0.999, and its calculated q_e values agree with the experimental q_e values. This confirms that the adsorption data are well represented by the pseudo-second-order kinetic model. From Table 2, it was observed that the intraparticle diffusion rate constant increased with an increase in initial Direct Red 23 concentrations.

Table 2: Pseudo-first-order, pseudo-second-order, and intraparticle diffusion models rate constants and calculated equilibrium from experimental data.

Kinetic models	Ce (mg/l)	
	50	100
q_e exp	12.08	20.51
Pseudo-first-order		
q_e cal	1.08	3.87
k_1 (1/min)	4.49×10^{-2}	2.42×10^{-2}
R^2	0.9748	0.9924
Pseudo-second-order		
q_e cal	12.14	20.75
k^2 (g/mg min)	1.35×10^{-1}	1.9×10^{-2}
R^2	1	0.9993
Intraparticle diffusion		
K_p (mg/g min ^{0.5})	0.0931	0.4135
C	11.23	16.25
R^2	0.8228	0.9725

3.4 Thermodynamic Parameters

Spontaneity of a process can be determined by thermodynamic parameters such as enthalpy change (ΔH°), free energy change (ΔG°) and entropy change (ΔS°). A spontaneous process will show a decrease in ΔG° and ΔH° values with increasing temperature.¹⁹ The temperatures used in the thermodynamic study were 303, 318 and 333 K. The thermodynamic parameters were calculated based on the following equations:

$$\Delta G^\circ = \Delta H^\circ - T\Delta S^\circ \quad (10)$$

$$\ln b = \frac{\Delta S^\circ}{R} - \frac{\Delta H^\circ}{RT} \quad (11)$$

where b is the equilibrium constant, R is the universal gas constant (8.314 J/mol K), and T is the temperature (K). Table 3 lists down the values for the thermodynamic parameters. The positive value for the enthalpy change, ΔH° (13.10 kJ/mol), indicates the endothermic nature of the adsorption, which

explains the increase of Direct Red 23 adsorption efficiency as the temperature increased. The positive value for the entropy change, ΔS° (136.91 J/mol K), indicates that there is an increased disorder at the solid/liquid interface during Direct Red 23 adsorption onto the MGA. The negative value for the free energy change, ΔG° , implies the spontaneity of the adsorption process, which does not require an external energy source for the system.

Table 3: Thermodynamic parameters.

Temperature (K)	Thermodynamic parameters		
	ΔG° (kJ/mol)	ΔH° (kJ/mol)	ΔS° (J/mol K)
303	-28.67		
318	-30.51	7.291	118.75
333	-32.23		

4. CONCLUSION

The MGA functional groups and surface texture were successfully characterised using FTIR, SEM-EDX and pH_{zpc} modification. The experimental data for the adsorption of Direct Red 23 onto the MGA were well described by the Langmuir isotherm model, with a maximum adsorption capacity of 26.67 mg/g. The adsorption of Direct Red 23 was found to follow pseudo-second-order kinetics. Thermodynamic parameters such as enthalpy change (ΔH°), free energy change (ΔG°) and entropy change (ΔS°) showed that the adsorption process of Direct Red 23 was endothermic and spontaneous. The results show that *Uncaria gambir* has the potential to be developed into an effective adsorbent for the removal of Direct Red 23 from aqueous solution.

5. ACKNOWLEDGEMENTS

The authors gratefully acknowledge the research grant provided by the Universiti Sains Malaysia (No.1001/PKIMIA/833015) and a USM Fellowship for financial support of this work.

6. REFERENCES

1. Marsh, H. & Rodríguez-Reinoso, F. (2006). *Activated carbon*. Amsterdam: Elsevier.
2. Noroozi, B., Sorial, G. A., Bahrami, H. & Arami, M. (2007). Equilibrium and kinetic adsorption study of a cationic dye by a natural adsorbent-Silkworm pupa. *J. Haz. Mater.*, B139, 167–174.
3. Reife, A. (1993). Dyes, environmental chemistry. In Kirk-Othmer (Ed.). *Encyclopedia of chemical technology*. Washington: John Wiley & Sons, 753.
4. Pagga, U. & Braun, D. (1986). The degradation of dye stuffs: part II. Behaviour of dyestuffs in aerobic biodegradation tests. *Chemosphere*, 154, 79–489.
5. Lahaye, J. (1998). The chemistry of carbon surfaces. *Fuel*, 77(6), 543–547.
6. Yenisoy-Karakas, S., Aygun, A., Gunes, M. & Tahtasakal, E. (2004). Physical and chemical characteristics of polymer-based spherical activated carbon and its ability to adsorb organics. *Carbon*, 42, 477–484.
7. Dursun, O., Gu'lbeyi, D. & Ahmet, O. (2007). Methylene blue adsorption from aqueous solution by dehydrated peanut hull. *J. Haz. Mater.*, 144, 171–179.
8. Robinson, T., McMullan, B., Chandran, R. & Nigam, O. (2002). Effect of pretreatments of three waste residues, wheat straw, corncobs and barley husks on dye adsorption. *Bioresour. Technol.*, 85, 119–124.
9. Renmin, G., Yi, D., Mei, L., Chao, Y., Huijun, L. & Yingzhi, S. (2005). Utilization of powdered peanut hull as biosorbent for removal of anionic dyes from aqueous solution. *Dyes Pigments*, 64, 187–192.
10. Gurusamy, A. & Jiunn-Fwu, L. (2008). Equilibrium studies on the adsorption of acid dye into chitin. *Environ. Chem Lett.*, 6, 77–81.
11. Franca, A. S., Oliveira, L. S. & Ferreira, M. E. (2009). Kinetics and equilibrium studies of methylene blue adsorption by spent coffee ground. *Desalination*, 249, 267–272.
12. Tamez, U. M., Akhtarul, I. M., Shaheen, M. & Rukanuzzaman, M. (2009). Adsorptive removal of methylene blue by tea waste. *J. Haz. Mater.*, 164, 53–60.
13. Mokhtar, A., Nargess, Y. L., Niyaz, M. M. & Nooshin, S. T. (2005). Removal of dyes from colored textile wastewater by orange peel adsorbent: Equilibrium and kinetic studies. *J. Coll. Interf. Sci.*, 288, 371–376.
14. Ola, A., Ahmed, E. N., Amany, E. S. & Azza, K. (2005). Use of rice husk for adsorption of direct dyes from aqueous solution: A case study of direct F. Scarlet. *Egyptian J. Aquatic Res.*, 31(1), 1–11.

15. Tan, L. S., Jain, K. & Rozaini, C. A. (2010). Adsorption of textile dye from aqueous solution on pretreated mangrove bark, an agricultural waste: Equilibrium and kinetic studies. *J. App. Sci. Environ. Sani.*, V(N), 266–276.
16. Kavitha, D. & Namasivayam, C. (2007). Experimental and kinetic studies on methylene blue adsorption by coir pith carbon. *Biores. Tech.*, 98, 14–21.
17. Hazwan, M. & Jain, K. (2010). Electrochemical studies of mild steel corrosion inhibition in aqueous solution by *Uncaria gambir* Extract. *J. Phy. Sci.*, 21(1), 1–13.
18. Garro-Galvez, J. M., Fechtal, M. & Riedl, B. (1996). Gallic acid as a model of tannins in condensation with formaldehyde. *Thermochim. Acta*, 274, 149–163.
19. Ngah, W. S. W. & Hanafiah, M. A. K. M. (2008). Adsorption of copper on rubber (*Hevea brasiliensis*) leaf powder: Kinetic, equilibrium and thermodynamic studies. *Biochem. Eng. J.*, 39, 521–530.
20. Langmuir, I. (1918). The adsorption of gases on plane surfaces of glass, mica, and platinum. *J. Am. Chem. Soc.*, 40, 1361–1367.
21. Weber, T. W. & Chakkravorti, R. K. (1974). Pore and solid diffusion models for fixed bed adsorbers. *Amer. Inst. Chem. J.*, 20, 228.
22. Freundlich, H. (1907). Ueber die adsorption in Loesungen. *Z. Phys. Chem.*, 57, 385–470.
23. Temkin, M. J. & Pyzher, V. (1940). Recent modifications to Langmuir isotherms. *Acta Physicochem.*, 12, 217–222.
24. Tong, K. S., Jain, K. M. & Azraa, A. (2011). Adsorption of copper ion from its aqueous solution by a novel biosorbent *Uncaria gambir*: Equilibrium, kinetics, and thermodynamic studies. *Chem. Eng. J.*, 170(1), 145–153.
25. McKay, G., Blair, H. & Gardiner, J. R. (1989). The adsorption of dyes onto chitin in fixed bed column and batch absorbers. *J. Appl. Polym. Sci.*, 28, 1499–1544.
26. Weber, W. J. & Morris, J. C. (1963). Kinetics of adsorption on carbon from solution. *J. Sanitary Eng. Div. Proceed. Am. Soc. Civil Eng.*, 89, 31–59.
27. Kannan, N., Sundaram, M. M. (2001). Kinetics and mechanism of removal of methylene blue by adsorption on various carbons – a comparative study. *Dyes and Pigments*, 51, 25–40.